A Lorenz/Boer energy budget for the atmosphere of Mars from a "reanalysis" of spacecraft observations

Journal Item

Supporting Information for "A Lorenz/Boer energy budget for the atmosphere of Mars from a reanalysis of spacecraft observations"

Contents of this file

Corresponding author: F. Tabataba-Vakili, Atmospheric, Oceanic and Planetary Physics, Department of Physics, University of Oxford, UK. (tabataba-vakili@atm.ox.ac.uk)

7. Integrands of the energy and conversion terms resolved over latitude and pressure (Fig. S4)

8. Diurnal component of the integrands shown in Fig. S4 (Fig. S5)

9. Time-resolved total, daily averaged and diurnal components of the conversion terms on the northern hemisphere of Mars (Fig. S6)

10. Time-resolved total, daily averaged and diurnal components of the conversion terms on the southern hemisphere of Mars (Fig. S7)

Introduction

The Lorenz budget equations presented in the paper (equations 1 - 4) are solved according to *Boer* [1989] by:

$$K_Z = \int_M \frac{1}{2}[\Theta][\boldsymbol{V}]_R \cdot [\boldsymbol{V}]_R dm \tag{1}$$

$$K_E = \int_M \frac{1}{2}[\Theta \boldsymbol{V}^* \cdot \boldsymbol{V}^*] dm \tag{2}$$

$$\begin{aligned} A_Z &= A_{Z1} + A_{Z2} \\ &= \int_M C_p \Theta N_Z [T]_R dm + \int_S (p_s - \pi_{sZ}) \Phi_s d\sigma / g \end{aligned} \tag{3}$$

$$\begin{aligned} A_E &= A_{E1} + A_{E2} \\ &= \int_M C_p \Theta (N - N_Z) T dm + \int_S (\pi_{sZ} - \pi_s) \Phi_s d\sigma / g \end{aligned} \tag{4}$$

$$\begin{aligned} C_K &= C_{K1} + C_{K2} \\ &= -\int_M a \cos\phi \left\{ \left([\Theta u^* \boldsymbol{V}^*] \cdot \nabla + [\Theta u^* \omega^*] \frac{\partial}{\partial p} \right) \right. \\ &\qquad \left(\frac{[u]_R}{a \cos\phi} \right) \cdot \left([\Theta v^* \boldsymbol{V}^*] \cdot \nabla + [\Theta v^* \omega^*] \frac{\partial}{\partial p} \right. \\ &\qquad \left. \left. -\frac{\tan\phi}{a} [\Theta \boldsymbol{V}^* \cdot \boldsymbol{V}^*] \right) \left(\frac{[v]_R}{a \cos\phi} \right) \right\} dm \\ &\quad + \int_M \left\{ \left[\Theta \frac{\partial \Phi^*}{\partial t} \right] + [\boldsymbol{V}]_R \cdot [\Theta \nabla \Phi^*] \right. \\ &\qquad \left. + [\omega]_R \left[\Theta \frac{\partial \Phi^*}{\partial p} \right] \right\} dm \end{aligned} \tag{5}$$

$$C_Z = C_{Z1} + C_{Z2}$$

$$= -\int_M [\Theta][\omega]_R[\alpha]_R dm - \int_S \left[\frac{\partial p_s}{\partial t}\Phi_s\right] d\sigma/g \tag{6}$$

$$C_E = -\int_M [\Theta\omega^*\alpha^*] dm \tag{7}$$

$$C_A = -\int_M C_p \left(\frac{\theta}{T}\right)\left([\Theta T^*\boldsymbol{V}^*]\cdot\nabla + [\Theta T^*\omega^*]\frac{\partial}{\partial p}\right) \left(\frac{T}{\theta}N_Z\right) dm \tag{8}$$

$$G_Z = \int_M \Theta N_Z [Q]_R dm \tag{9}$$

$$G_E = \int_M \Theta(N - N_Z) Q dm \tag{10}$$

$$F_Z = \int_M [\Theta][\boldsymbol{V}]_R \cdot [\boldsymbol{F}] dm \tag{11}$$

$$F_E = -\int_M [\Theta\boldsymbol{V}^*\cdot\boldsymbol{F}^*] dm \tag{12}$$

with

$$\Theta(p - p_s) = \Theta(\lambda, \phi, p, t) = \begin{cases} 1, & p < p_s \\ 0, & p > p_s \end{cases} \tag{13}$$

$$[X]_R = \begin{cases} [\Theta X]/[\Theta], & [\Theta] \neq 0 \\ [X], & [\Theta] = 0 \end{cases} \tag{14}$$

$$X^* = X - [X]_R \tag{15}$$

$$N(\pi) = 1 - (\pi/p)^\kappa \tag{16}$$

$$N_Z = N(\pi_Z) \tag{17}$$

$$\pi_Z = \pi([\theta]_R, t) \tag{18}$$

$$[\theta]_R = [T]_R \left(\frac{p_{00}}{p}\right)^\kappa \tag{19}$$

$$\nabla = \begin{pmatrix} \partial_x \\ \partial_y \end{pmatrix} = \begin{pmatrix} \frac{1}{a\cos\phi}\partial_\lambda \\ \frac{1}{a}\partial_\phi \end{pmatrix} \tag{20}$$

and

A_E: eddy available potential energy

A_Z: zonal available potential energy

C_A: conversion term between A_Z and A_E

C_E: conversion term between A_E and K_E

C_K: conversion term between K_Z and K_E

C_Z: conversion term between A_Z and K_Z

F_E: dissipation of K_E by friction

F_Z: dissipation of K_Z by friction

G_E: generation of A_E by diabatic heating

G_Z: generation of A_Z by diabatic heating

K_E: eddy kinetic energy

K_Z: zonal kinetic energy

$[X]$: zonal mean of X

N: efficiency factor

N_Z: zonal efficiency factor

p_s: surface pressure

$\boldsymbol{V}$: horizontal velocity vector field

u: zonal component of $\boldsymbol{V}$

v: meridional component of $\boldsymbol{V}$

α: specific volume $(1/\rho)$

$\hat{\theta}_s$: potential at k-th isentropic level of the reference state

κ: R/c_p

π: pressure of the reference state

π_{sZ}: zonal-mean of surface pressure of the reference state

ρ: density

Φ: geopotential

Φ_s: surface geopotential

ω: vertical velocity vector in pressure coordinates

Q: heating rate

F: dissipation of kinetic energy

Θ: Heaviside step function

Text S1.

Figure S4 shows the integrands of the altitude-dependent energy and conversion terms in longitudinal and temporal mean, plotted over latitude and pressure. K_Z shows strong contributions in mid-latitudes, coinciding with jet activities. K_E values seem to be correlated with K_Z, except for a region in the upper atmosphere of the south-polar region. Further analysis shows that this maximum receives most of its contribution during the GDSE of MY 25. The integrands of A_{Z1} mirror the behaviour (and sign) of the zonal-mean efficiency factor N_Z by showing negative regions in the in the pole regions, this pattern is also observed in the Earth atmosphere [see e.g. *Siegmund*, 1994, , their Figure 3]. Please note that the effect of using the efficiency factor to determine APE integrands is signifi-

cant [see *Boer*, 1975]. A_{E1} shows non-zero values at the surface, extending latitudinally towards the upper mid-latitudes. A temporal analysis (not shown) reveals that large A_{E1} integrands are found to coincide with strongly negative A_{Z1} integrands, revealing maxima in the difference between N and N_Z.

The bottom half of Figure S5 shows the integrands of the conversion terms. Please note that most of the visible patterns displayed have only small contributions to the integrated values presented above because the mass element dm strongly favours lower altitudes. C_A, just like K_Z and A_{Z1}, is stronger in the northern hemisphere. The maximum of C_A in the north polar region coincides with NH winter, and thereby with the extrema of K_Z and A_{Z1}. C_E has positive (A_E to K_E) integrands in the equatorial region and negative (K_E to A_E) values polar regions and high altitudes. The negative values seem slightly correlated to regions with high K_E. The visible pattern of C_{K1} is strongly correlated with the south polar maximum in K_E that occurs during the GDSE. The global-mean values of C_{K1} originate from lower altitudes because these are more strongly weighted. We find that maxima of C_{K2} coincide with high values of A_Z in the southern hemisphere. C_{Z1} shows thermally direct circulation in the summer hemisphere and thermally indirect circulation in the winter hemisphere. The annual mean shows that the southern summer circulation dominates.

An evaluation of the diurnal components (Fig. S5) of these integrands shows correlating patterns for those terms that are strongly affected by diurnal timescales (i.e. K_E, A_{E1}, C_A, C_E, C_{K1}) and generally negligible diurnal integrands for the rest.

References

Boer, G. J. (1975), Zonal and eddy forms of the available potential energy equations in pressure coordinates, *Tellus*, *27*(5), 433–442.

Boer, G. J. (1989), On exact and approximate energy equations in pressure coordinates, *Tellus A*, *41*(2), 97–108.

Boer, G. J., and S. Lambert (2008), The energy cycle in atmospheric models, *Climate dynamics*, *30*(4), 371–390.

Siegmund, P. (1994), The generation of available potential energy, according to lorenz exact and approximate equations, *Tellus A*, *46*(5), 566–582.

	$L_s[^\circ]$	A_Z [10^5 J/m^2]	A_E	K_Z [10^5 J/m^2]	K_E	C_A [W/m^2]	C_E	C_K [W/m^2]	C_Z	C_{K1} [W/m^2]	C_{K2}	C_{Z1} [W/m^2]	C_{Z2}
	0-90	10.8	0.74	0.29	0.08	0.04	0.07	0.02	0.16	-0.003	0.020	0.16	-0.002
	90-180	10.3	0.76	0.24	0.08	0.02	0.07	0.01	0.10	-0.004	0.019	0.09	0.009
global	180-270	14.2	0.68	0.71	0.23	0.07	0.17	0.04	-0.07	0.033	0.012	-0.06	-0.014
	270-360	7.6	0.66	0.66	0.15	0.06	0.11	0.04	-0.03	0.021	0.017	-0.03	0.008
	annual	10.6	0.72	0.44	0.13	0.04	0.11	0.02	0.05	0.009	0.016	0.05	5E-4
	0-90	20.0	0.58	0.21	0.09	0.04	0.09	0.02	1.77	-0.004	0.022	1.78	-0.002
	90-180	18.5	0.62	0.12	0.08	0.01	0.07	0.02	1.10	0.001	0.018	1.08	0.02
NH	180-270	9.91	0.53	1.22	0.20	0.10	0.16	0.04	-7.36	0.064	-0.022	-7.33	-0.04
	270-360	3.71	0.48	1.15	0.19	0.11	0.14	0.04	-4.64	0.041	-0.006	-4.66	0.02
	annual	13.7	0.55	0.61	0.13	0.06	0.11	0.03	-1.90	0.022	0.005	-1.90	2E-4
	0-90	1.16	0.90	0.38	0.08	0.03	0.05	0.02	-1.45	-0.003	0.019	-1.45	-0.002
	90-180	2.17	0.93	0.36	0.08	0.03	0.07	0.01	-0.90	-0.008	0.019	-0.90	0.002
SH	180-270	18.5	0.82	0.20	0.25	0.03	0.18	0.05	7.21	0.001	0.045	7.20	0.01
	270-360	11.5	0.83	0.17	0.11	0.01	0.09	0.03	4.59	0.001	0.034	4.59	-0.004
	annual	7.54	0.88	0.28	0.14	0.03	0.10	0.02	2.00	-0.003	0.027	2.00	0.001

Table S1. Lorenz energy budget of Mars in seasonal and hemispheric decomposition. Seasons are given in solar longitudes, where $L_s = 0^\circ$ is northern hemisphere spring equinox. Hence e.g. $L_s = 0 - 90^\circ$ is spring on the northern hemisphere, followed by summer, autumn and winter. Annual values were averaged over two full years (MY 25 and MY 26). Seasonal values are the mean of either two ($L_s = 0 - 180^\circ$) or three ($L_s = 180 - 360^\circ$) full seasons .

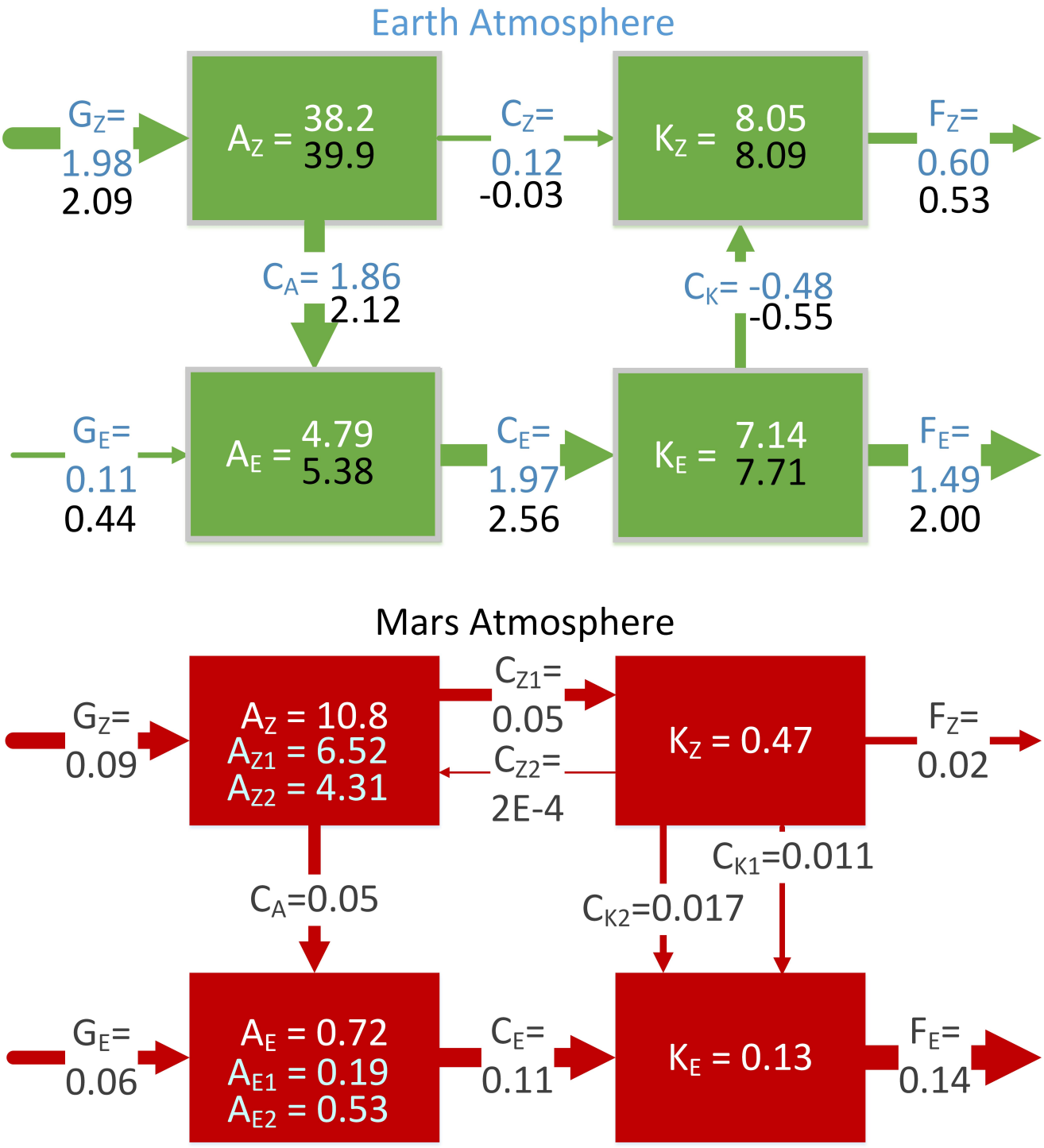

Figure S1. Mean values of energy and conversion terms per unit area of Earth (top, *Boer and Lambert* [2008]) from NCEP (white/blue) and ERA(black) reanalysis data over 17 years (1979-1995); of Mars over almost 3 martian years (bottom, current work) . All Energies (A_Z,A_E,K_Z,K_E) are given in 10^5 Jm^{-2} and all conversion terms in Wm^{-2}.

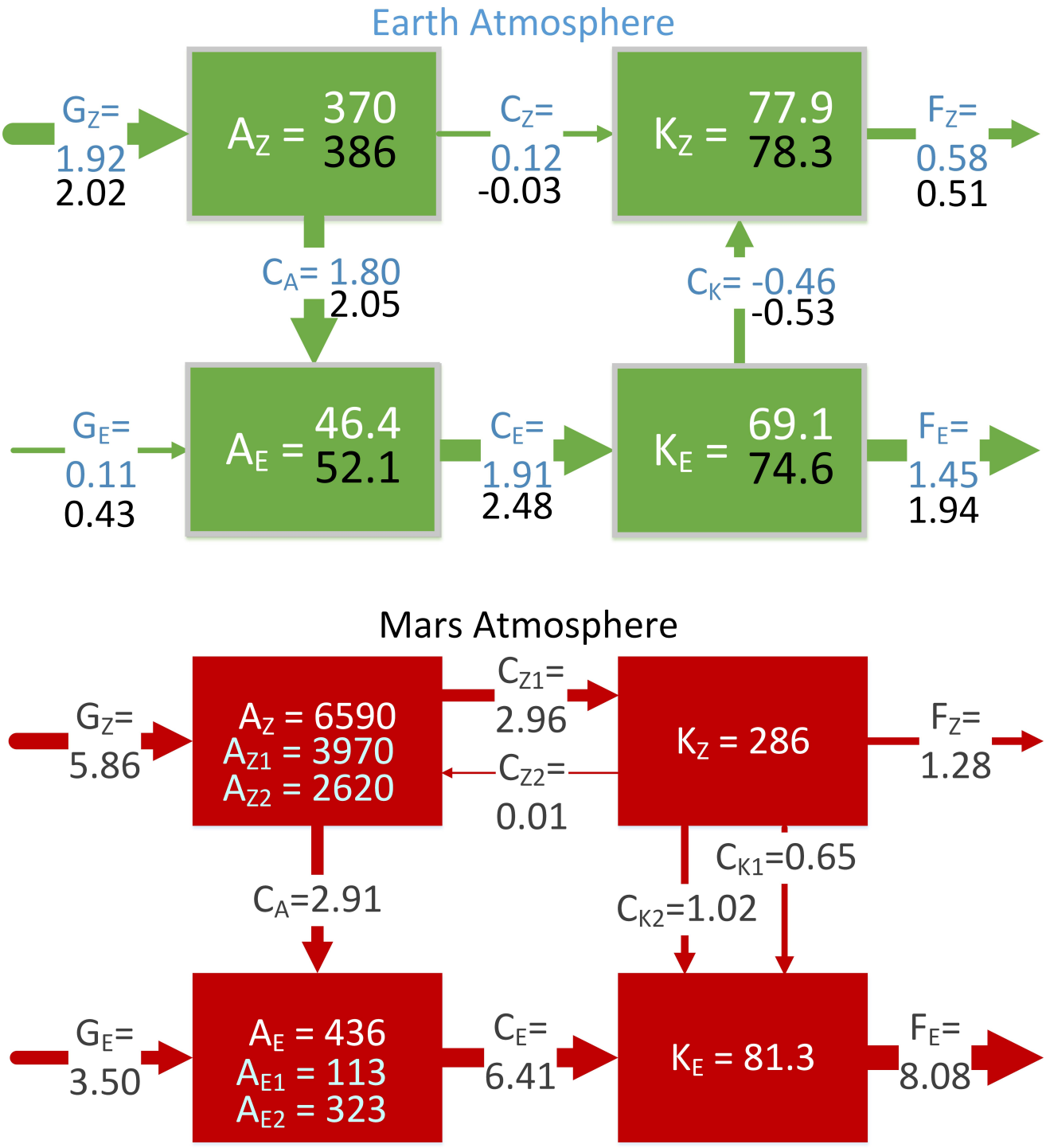

Figure S2. Mean values of energy and conversion terms per unit mass of Earth (top, *Boer and Lambert* [2008]) from NCEP (white/blue) and ERA(black) reanalysis data over 17 years (1979-1995); of Mars over almost 3 martian years (bottom, current work) . All Energies (A_Z,A_E,K_Z,K_E) are given in J/kg and all conversion terms in 10^{-5} W/kg.

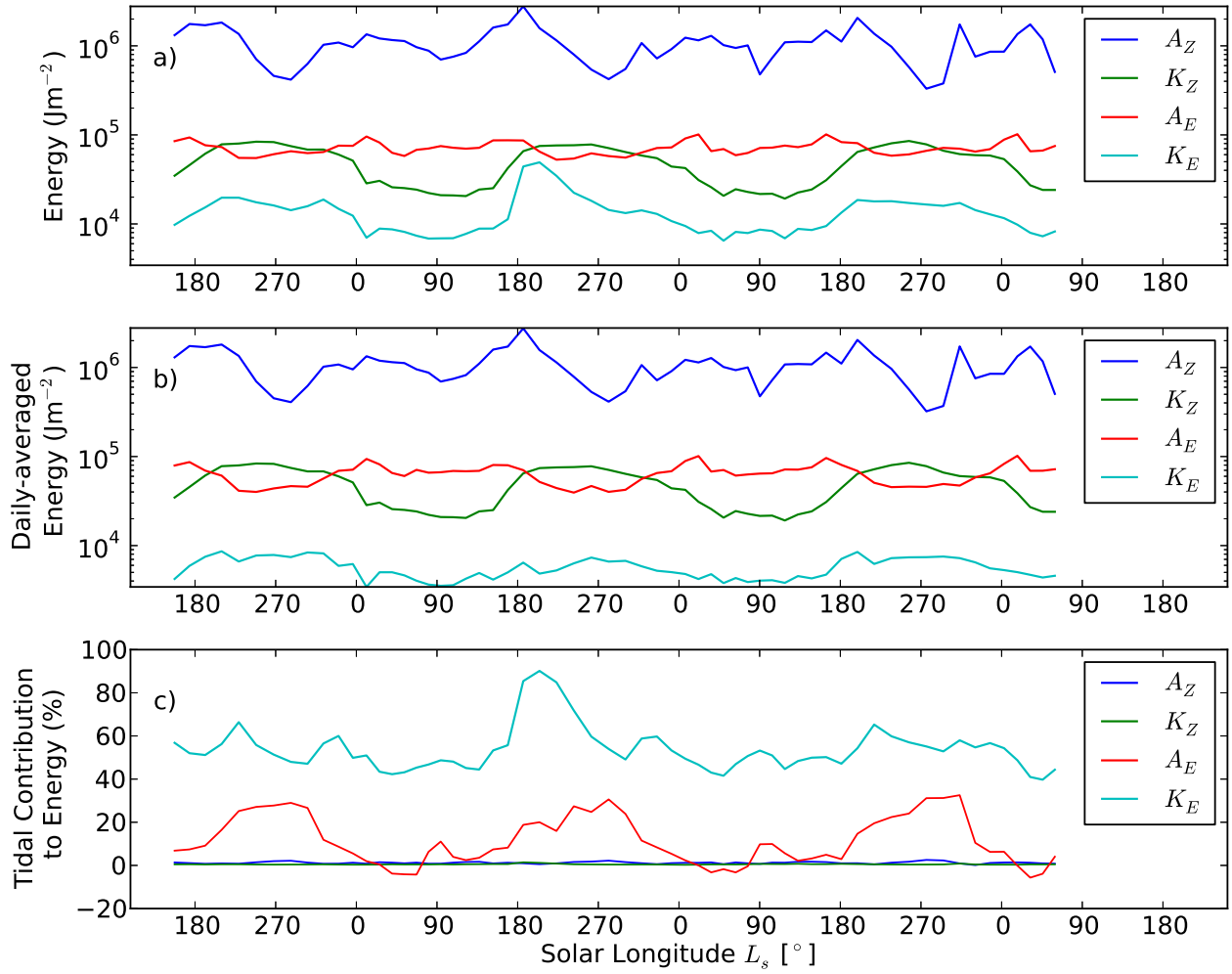

Figure S3. Total (a), daily averaged (b) and tidal (c) component of the conversion terms of the Lorenz energy budget of the Mars atmosphere given in 30-sol mean values from $L_s = 141°$ MY 24 to $L_s = 82°$ MY 27. The tidal component (c) shows the contribution ($X_{\text{tidal}}/X \cdot 100\%$) of the tidal component to the total energies in percent.

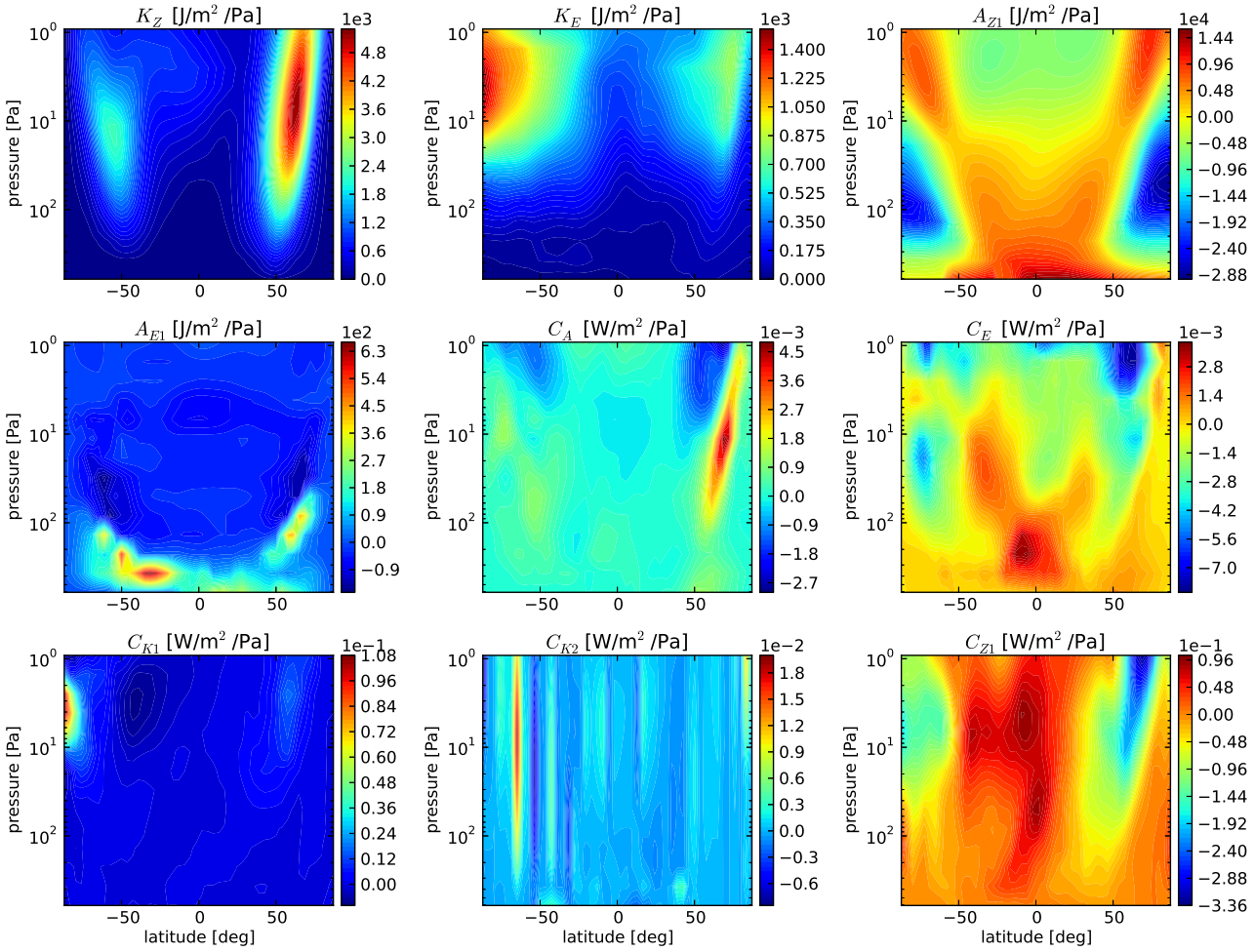

Figure S4. Integrands of energy and conversion terms resolved over latitude and pressure coordinates. Displayed data is a mean over two full martian years.

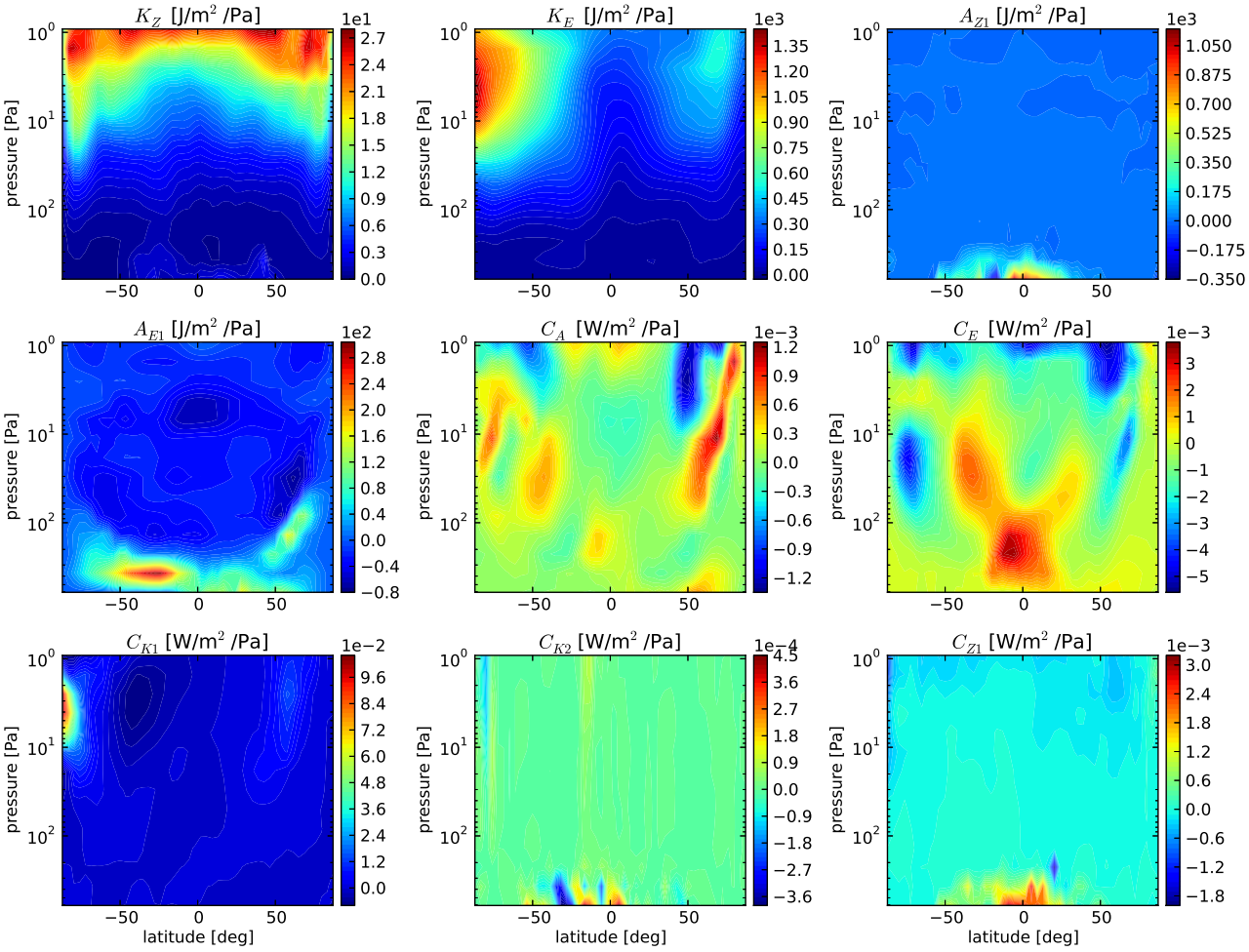

Figure S5. Diurnal components of the integrands of energy and conversion terms resolved over latitude and pressure coordinates. Displayed data is a mean over two full martian years.

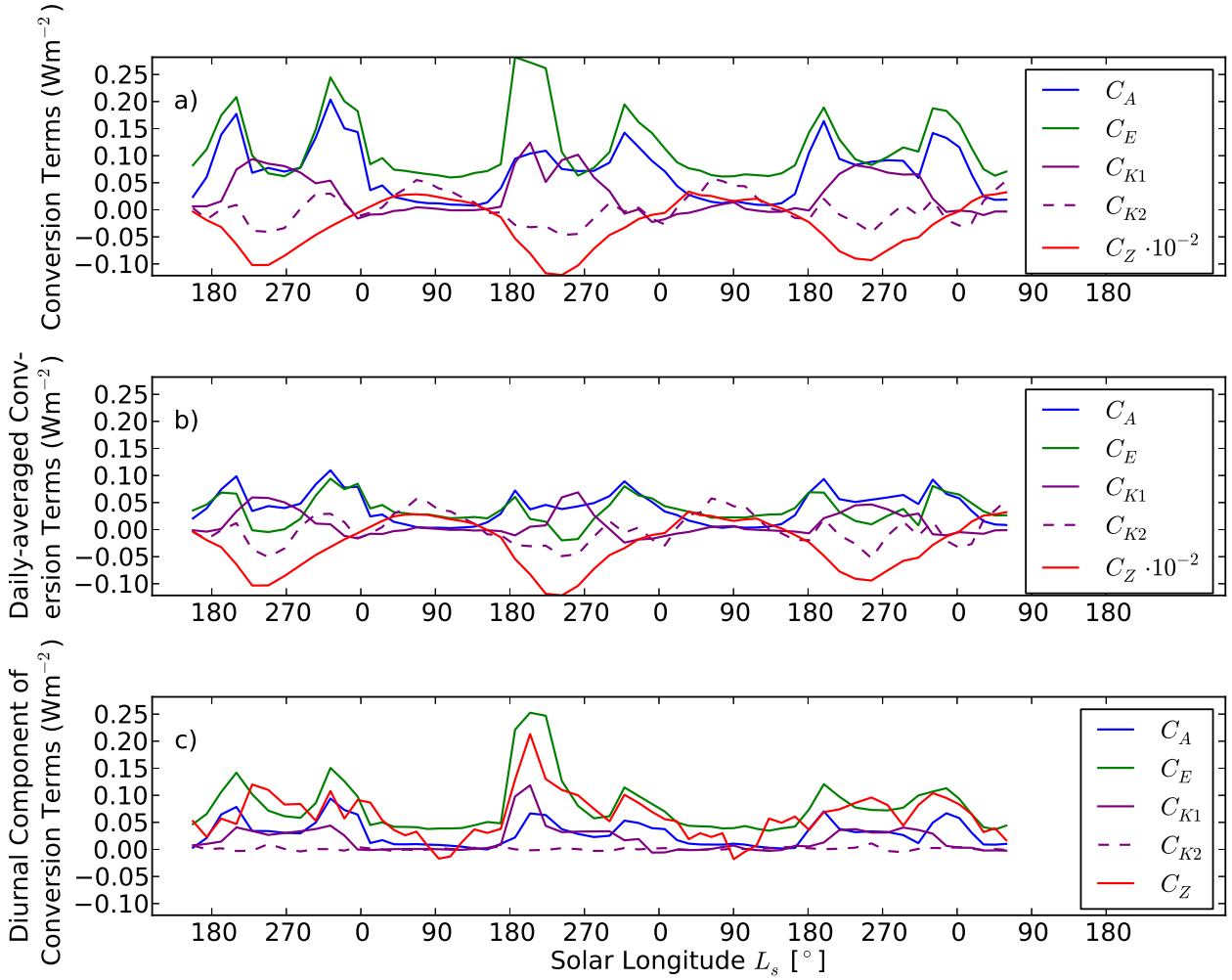

Figure S6. Total (a), daily averaged (b) and tidal (c) component of the conversion terms of the Lorenz energy budget of the northern hemisphere of the Mars atmosphere given in 30-sol mean values from $L_s = 141°$ MY 24 to $L_s = 82°$ MY 27.

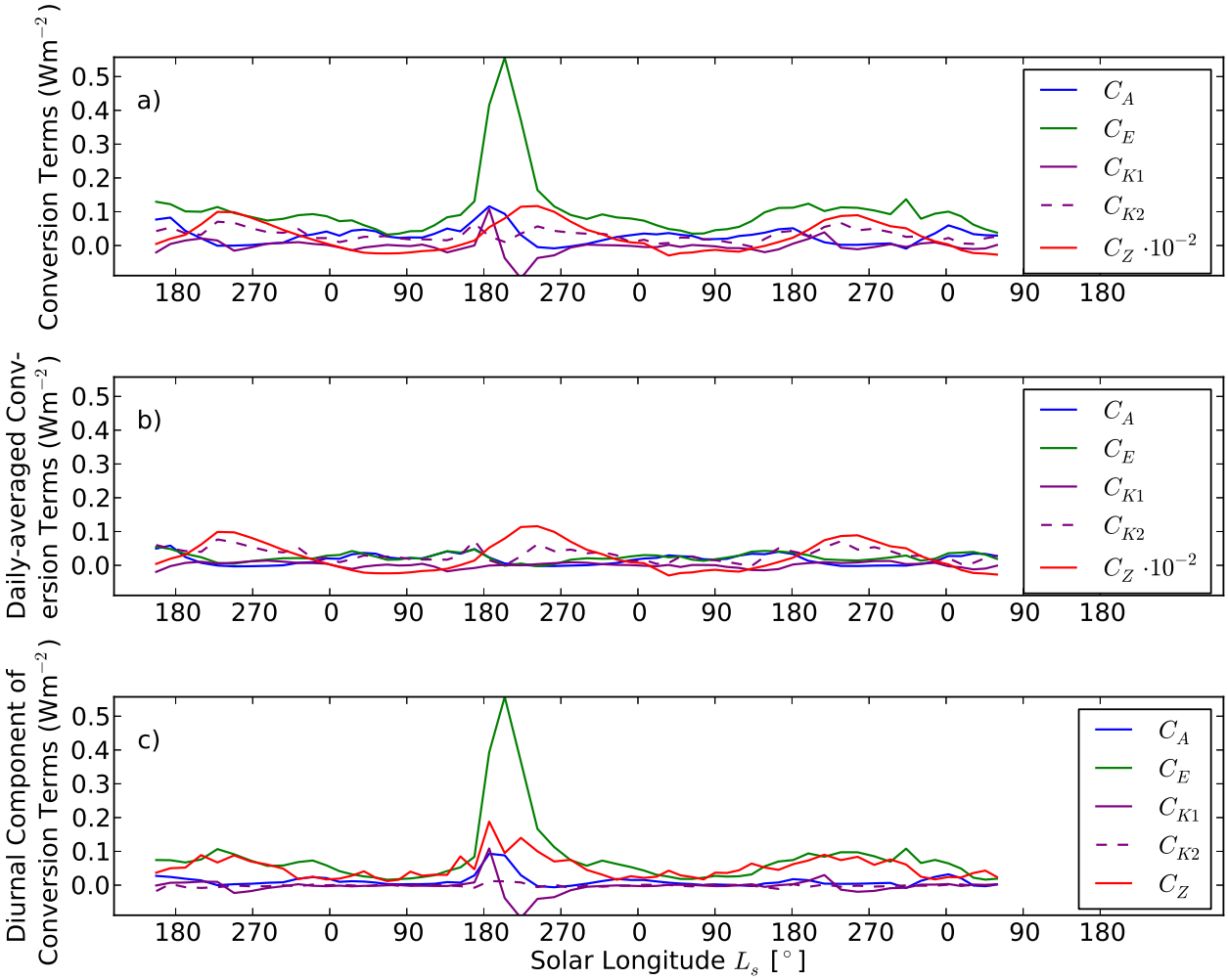

Figure S7. Total (a), daily averaged (b) and tidal (c) component of the conversion terms of the Lorenz energy budget of the southern hemisphere of the Mars atmosphere given in 30-sol mean values from $L_s = 141°$ MY 24 to $L_s = 82°$ MY 27.